PADÉ-BASED INTERPRETATION AND CORRECTION OF THE GIBBS PHENOMENON

TOBIN A. DRISCOLL* AND BENGT FORNBERG†

Abstract. The convergence of a Fourier series on an interval can be interpreted naturally as the convergence of a Laurent series on the unit circle in the complex plane. In turn this Laurent series can be interpreted as the sum of an analytic and a co-analytic Taylor series.The Gibbs phenomenon in this context can be seen as an attempt to approximate a logarithmic branch cut with such series. Conversion of a truncated Taylor series to a Padé approximation does a much better job of approximating on most of the unit circle, but a rational function cannot approximate the jump itself. However, one can modify the traditional Padé approximation to include logarithmic singularities. When the jump locations are known exactly, this process appears to converge exponentially to a discontinuous or nonsmooth function throughout the interval . When the jump locations are not known in advance, standard Padé approximation to the derivative of the original series gives poles that approximate jump locations to what is observed to be fourth-order accuracy. All the procedures have analogs in the case of trigonometric interpolation of equispaced data.

1. Introduction. From the standpoint of computation, the Gibbs phenomenon is often an obstacle to be overcome. Truncated Fourier series, or trigonometric interpolants, exhibit spectral (exponential) convergence to functions that are analytic on and near the real axis. However, for a C^p piecewise continuous function, the convergence is reduced to the algebraic rate $O(N^{-p-1})$ when N terms are kept [18]. As continuous functions, trigonometric polynomials can be expected to have trouble representing jumps and corners. But the greatly reduced convergence occurs globally, not just near the locations of jumps. (Henceforth we use the term "jumps" to include jumps in value and/or one or more derivatives.)

Many remedies to the reduced convergence can be found in the literature. Broadly speaking, there are two major tasks: finding the location(s) of jumps, and correcting for their effects. The latter problem, which seems to be easier than the former, is addressed by Eckhoff in [7] by using linear least-squares fitting for coefficients of extra jump terms added to the Fourier series. In [10] (and references therein), Gottlieb and Shu prove spectral reconstruction on subintervals of analyticity by least-squares projection onto spaces of Gegenbauer polynomials with weights that vary with N, though a subsequent study by Boyd [3] suggests that this method can run into a Runge-like instability in practice. The Gegenbauer idea was much improved by Shizgal and Jung in [14]. Tanner [17] uses a filter whose support is optimally adjusted in both space and dual space to recover exponential convergence in intervals of analyticity, though he acknowledges that accurate reconstruction near jumps is not possible with this method. The more difficult task of reconstruction without prior knowledge of jump locations is attempted by nonlinear optimization in [7] and [12]. Gelb and Tadmor [9] use filtering to simultaneously recover jump locations and sizes, to an accuracy of $O(\log N/N)$.

We will investigate the convergence issue using a natural connection between Fourier series on the real line and Laurent series in the complex plane. Let $f(x)$ be piecewise analytic for $x \in [-\pi, \pi)$. While we do not assume that f is 2π-periodic, the Fourier series of f implicitly extends f periodically. A lack of native periodicity is thus equivalent to discontinuities in f and all its derivatives at $x = -\pi$. The Fourier

*Department of Mathematical Sciences, University of Delaware, Newark, DE 19716, USA

†University of Colorado, Department of Applied Mathematics, 526 UCB, Boulder, CO 80303, USA. Supported by NSF Grant DMS-0309803.

series for f is given by

$$f(x) = \sum_{n=-\infty}^{\infty} c_n e^{inx}, \qquad c_n = \frac{1}{2\pi}\int_{-\pi}^{\pi} f(x)e^{-inx}\,dx. \tag{1.1}$$

If f is real, then $c_{-n} = \bar{c}_n$. The transformation $z = e^{ix}$ maps the interval $[-\pi, \pi)$ to the unit circle in z. The Fourier expansion (1.1) becomes for the z-plane a Laurent expansion, which can be split into two parts:

$$f(z) = \sum_{n=-\infty}^{\infty} c_n z^n = \sum_{n=0}^{\infty}{}' c_n z^n + \sum_{n=0}^{\infty}{}' c_{-n} z^{-n} = f^+(z) + f^-\big(z^{-1}\big), \tag{1.2}$$

where the primed sums indicate that the zeroth term should be halved. If f is real, then we need only work with f^+ in practice, since on the unit circle we have

$$f^-\big(z^{-1}\big) = \sum_{n=0}^{\infty}{}' \bar{c}_n (\bar{z})^n = \overline{\sum_{n=0}^{\infty}{}' c_n z^n} = \overline{f^+(z)}. \tag{1.3}$$

Both f^+ and f^- are defined by Taylor expansions at the origin. Hence, questions about the partial Fourier sum

$$f_N(x) = \sum_{n=-N}^{N} c_n e^{inx}, \quad \text{or} \quad f_N(z) = \sum_{n=-N}^{N} c_n z^n, \tag{1.4}$$

are equivalent to questions about partial Taylor series for f^+ and f^-. If the trace of f on the unit circle has jumps, it is clear that f, and thus f^+ and f^-, will have singularities in the complex plane. It is hardly surprising, then, that their Taylor series converge very slowly.

Throughout this chapter, we will illustrate the statements and methods described using the four test functions shown in Table 1.1 and pictured in Figure 1.1. (The classical Gibbs examples $f(x) = \text{signum}(x)$ and $f(x) = x$ are not included because our methods ultimately reconstruct these examples exactly.)

TABLE 1.1
Test functions.

$f_a(x) = \exp\big(\sin(3x) + \cos(x)\big)$	Analytic and periodic
$f_b(x) = \exp\big(\sin(2.7x) + \cos(x)\big)$	Analytic but nonperiodic (jumps of all orders at $\pm\pi$)
$f_c(x) = \lvert x\rvert$	Continuous and periodic, with first-order jumps at $\pm\pi$
$f_d(x) = \begin{cases} \sin(x^2), & -\pi \le x < -\pi/3 \\ -e^{-2x}, & -\pi/3 < x < \pi/6 \\ 0, & \pi/6 < x < \pi/2 \\ 2 - x^2, & \pi/2 < x < \pi \end{cases}$	Jumps of multiple orders at four locations

The convergence of unaltered Fourier partial sums f_N is shown in Figure 1.2. Since the difference $f - f_N$ can be expected to have many zero crossings that are distracting

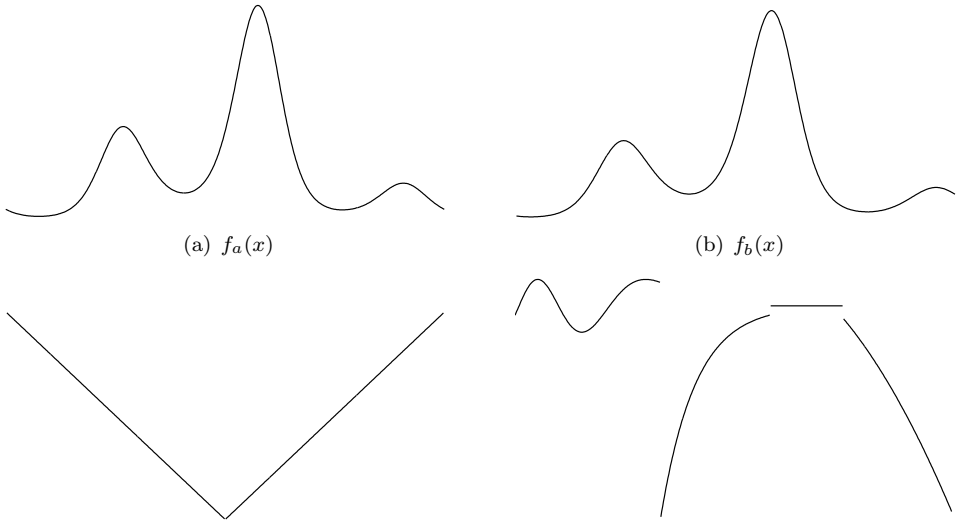

(a) $f_a(x)$ (b) $f_b(x)$

(c) $f_c(x)$ (d) $f_d(x)$

FIG. 1.1. *Test functions having zero, one, two, and four jump locations, respectively, including nonperiodicity (see Table 1.1).*

on a log scale, the error curves are smoothed by extracting all the local maxima of the absolute error, combined with the errors at irregular points, and connecting them to make a smooth envelope. For the analytic, periodic function f_a, the convergence is spectral—the curves are nearly equispaced as N increases uniformly (until double precision effects are felt near 10^{-16}). In the other cases, the convergence is globally slow.

Similar considerations arise when we deal with trigonometric interpolants instead of truncated Fourier series. Suppose we choose equispaced nodes

$$x_n = -\pi + \frac{2n+1}{2N}\pi, \qquad n = 0, 1, \ldots, 2N-1$$

and are given the $2N$ function samples $y_n = f(x_n)$. If we apply the discrete Fourier transform to $y_0, \ldots, y_{2N-1}$,

$$\tilde{c}_n = \frac{1}{2N} \sum_{m=0}^{2N-1} y_m e^{-inx_m}, \qquad n = -N, \ldots, N, \tag{1.5}$$

then $\tilde{c}_n$ is an approximation to the true Fourier coefficient c_n. The error in this approximation, called aliasing, results from the compression of infinitely many frequencies into the band-limited range that can be represented after discretization of space. If we replace c_n by $\tilde{c}_n$ in (1.4), the resulting $\tilde{f}_N$ is a trigonometric polynomial interpolating the $2N$ function samples.

Trigonometric interpolants suffer the same Gibbs phenomenon as truncated Fourier series. Correction of the phenomenon, however, is complicated by the aliasing error, which tends to mask the precise jump information that is implicit in the Fourier coefficients. One can again divide $\tilde{f}_N$ into analytic $\tilde{f}_N^+(z)$ and co-analytic $\tilde{f}_N^-(z^{-1})$. These are no longer truncated Taylor series, because their coefficients change with N, but their convergence behavior is similarly affected by jumps in the underlying f.

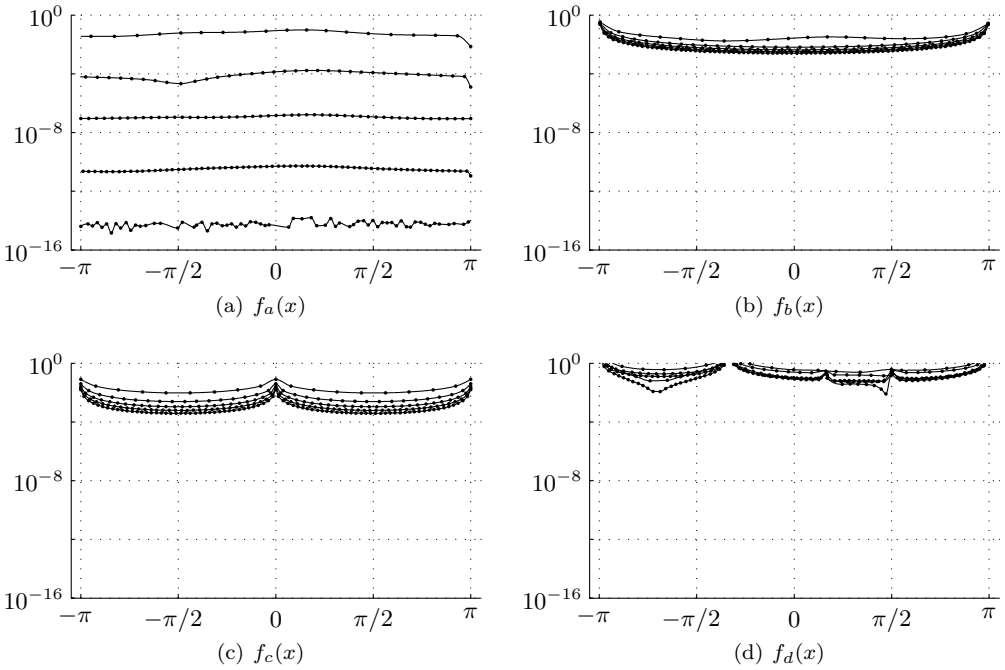

FIG. 1.2. *Error envelopes of Fourier partial sums for $N = 8, 16, 24, 32, 40$. (The points shown represent local maxima of the errors; these are connected to avoid distracting zero crossings of the true error.) Except for the analytic, periodic function f_a, the convergence is globally slow.*

In section 2 we review the classical technique of Padé approximation, which is a powerful tool for improving on the convergence of truncated Taylor series. Padé approximations define rational functions based on the truncated Taylor series. These approximations can converge rapidly while the underlying Taylor series converges poorly, or even diverges, as we will illustrate with an example. In section 3 we show that the Fourier–Padé technique [5, 8, 11, 16], in which Padé approximation is applied to f^+ and f^-, can indeed greatly improve upon the convergence of the original Fourier series to a function with jumps (or even to an analytic, periodic function). An analogous algorithm for the case of trigonometric interpolation is a rational interpolant, which is also demonstrated in section 3 to have a similar level of success. Still, the poles available in a rational approximation cannot reconstruct the jumps themselves, and small neighborhoods around the jumps resist convergence.

In section 4 we consider more carefully the structures that jumps in f on the unit circle cause in the complex plane. In fact, these jumps translate into logarithmic branch singularities in z. As was shown in [6], by adding the proper logarithmic terms into the Padé process, we can effectively restore spectral convergence throughout $[-\pi, \pi]$. This leads to an algorithm that we describe and test in section 5.

In section 6 we demonstrate that the Fourier–Padé idea can also be used for the problem of finding jump locations when they are unknown. By differentiating the original series, the logarithmic jump singularity is transformed into a pole that is accurately picked up by a standard Fourier–Padé approximation. Our experiments suggest that this technique can locate singularities from Fourier data with an error that is $O(N^{-4})$ in a difficult case. The method is not as successful in locating jumps

in equispaced sample values, however, presumably because of aliasing error in the Fourier coefficients.

2. Padé approximation. Given a formal power series expansion around zero, $\sum_{n=0}^{\infty} c_n z^n$, we define the type (M, N) Padé approximation by

$$P_M^N(z) = \frac{p(z)}{q(z)} = \frac{\displaystyle\sum_{n=0}^{N} a_n z^n}{\displaystyle\sum_{m=0}^{M} b_m z^m}, \tag{2.1}$$

where the coefficients of p and q are chosen so that the expansion of P_M^N matches the given series to as high an order as possible. Often one is most interested in the diagonal approximants P_N^N and the subdiagonal approximants P_{N+1}^N.

The normalization $b_0 = 1$ leaves $M + N + 1$ degrees of freedom in P_M^N. Thus, the coefficients should satisfy

$$\left(\sum_{n=0}^{M+N} c_n z^n\right)\left(\sum_{m=0}^{M} b_m z^m\right) - \left(\sum_{n=0}^{N} a_n z^n\right) = O(z^{M+N+1}). \tag{2.2}$$

The numerator p does not contribute to the terms beyond order N. Hence the coefficients for $z^{N+1}, \ldots, z^{M+N}$ in (2.2) yield the Toeplitz linear system

$$\begin{bmatrix} c_{N+1} & c_N & c_{N-1} & \cdots & c_{N+1-M} \\ c_{N+2} & c_{N+1} & c_N & \ddots & c_{N+2-M} \\ \vdots & \ddots & \ddots & \ddots & \vdots \\ c_{N+M} & \cdots & c_{N+2} & c_{N+1} & c_N \end{bmatrix} \begin{bmatrix} b_0 \\ b_1 \\ \vdots \\ b_M \end{bmatrix} = 0, \tag{2.3}$$

where we understand that $c_k = 0$ if $k < 0$. This $M \times (M + 1)$ linear system has nontrivial solutions. In most cases the normalization $b_0 = 1$ creates a unique solution. Once the coefficients of q are known, the numerator p is found through the terms of order N and less in (2.2). This gives $\mathbf{a} = C\mathbf{b}$, where $c_{ij} = c_{i-j}$. For example, if $N = M$, one obtains

$$\begin{bmatrix} a_0 \\ a_1 \\ \vdots \\ a_N \end{bmatrix} = \begin{bmatrix} c_0 & & & \\ c_1 & c_0 & & \\ \vdots & \ddots & \ddots & \\ c_N & \cdots & c_1 & c_0 \end{bmatrix} \begin{bmatrix} b_0 \\ b_1 \\ \vdots \\ b_M \end{bmatrix}. \tag{2.4}$$

Computing Padé approximants through linear algebra, as we have done here, is simple but not necessarily the most efficient or stable numerical method.

In Figure 2.1 we show how Padé approximation can accelerate the convergence of a power series. The left of the figure shows error curves on the unit circle $|z| = 1$ of diagonal Padé approximants $P_N^N(z)$ of the function e^z, for $N = 4, 8, 12, 16$. Exponential convergence is clear, up to the point for $N = 16$ that the error is comparable to machine precision. Of course, e^z is very well behaved in the complex plane, and the truncated Taylor series is exponentially convergent as well. Even so, the figure also shows that the Padé approximants are orders of magnitude more accurate than the series they are derived from.

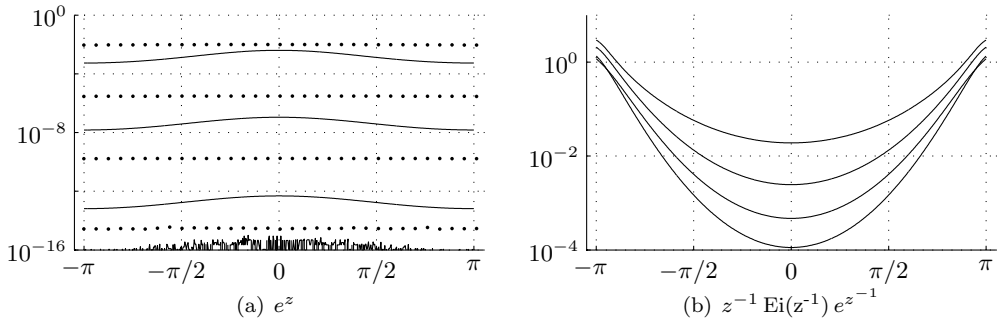

(a) e^z (b) $z^{-1}\,\mathrm{Ei}(z^{-1})\,e^{z^{-1}}$

FIG. 2.1. *Errors of diagonal Padé approximants P_N^N on the unit circle for $N = 4, 8, 12, 16$. In case (a), the function is entire and its series (whose errors shown by dots) converges exponentially, but the Padé approximants converge faster still. In case (b), the formal series is divergent away from the origin, but the Padé approximations again converge exponentially.*

More drastic still are the results on the right in Figure 2.1. These show the results of the same diagonal Padé approximants to

$$\int_0^\infty \frac{e^{-t}}{1+tz}\,dt = z^{-1}\,\mathrm{Ei}(z^{-1})\,e^{z^{-1}} \sim \sum_{n=0}^{\infty} n!(-z)^n,$$

where the asymptotic series is divergent for all $z \neq 0$. This function has a branch cut along the negative real axis, so its trace on the unit circle has a jump at $x = \pm\pi$. Nevertheless, the Padé approximants still converge exponentially, albeit slowly near the branch cut, as shown in the figure. In fact, exponential convergence in the cut plane is proven for all Stieltjes functions such as this one.

For a more thorough discussion of summation acceleration through Padé approximation, see [2, 15]. A comprehensive treatment of Padé approximation can be found in [1].

3. Fourier–Padé approximation. We return now to the context of Fourier series and their partial sums, as in (1.4). Recalling the splitting of f into f^+ and f^- in (1.2), we can convert their truncated Taylor series f_N^+ and f_N^- into Padé approximants. Specifically, we seek four polynomials $p^+(z)$, $q^+(z)$, $p^-(z)$, $q^-(z)$, each of degree $N/2$ for even N, such that

$$\begin{aligned} p^+(z) - q^+(z)f^+(z) &= O(z^{N+1}), \qquad z \to 0 \\ p^-(z) - q^-(z)f^-(z) &= O(z^{N+1}), \qquad z \to 0. \end{aligned} \tag{3.1}$$

If such polynomials can be found, the *Fourier–Padé* (FP) approximant to f is

$$f(x) \approx \frac{p^+(z)}{q^+(z)} + \frac{p^-(z^{-1})}{q^-(z^{-1})} = \frac{p^+(e^{ix})}{q^+(e^{ix})} + \frac{p^-(e^{-ix})}{q^-(e^{-ix})}. \tag{3.2}$$

Figure 3.1 displays the errors of Fourier–Padé approximants for the test functions in Table 1.1 and Figure 1.1. We observe dramatic improvement over the Fourier partial sums of Figure 1.2, even for the analytic and periodic function f_a. A Gibbs phenomenon still occurs at each jump, although the magnitude of the overshoot is observed to be about 2.5% instead of the usual 9% [16]. Unlike the case with Fourier partial sums, though, the convergence is not degraded globally. (In fact, it was shown

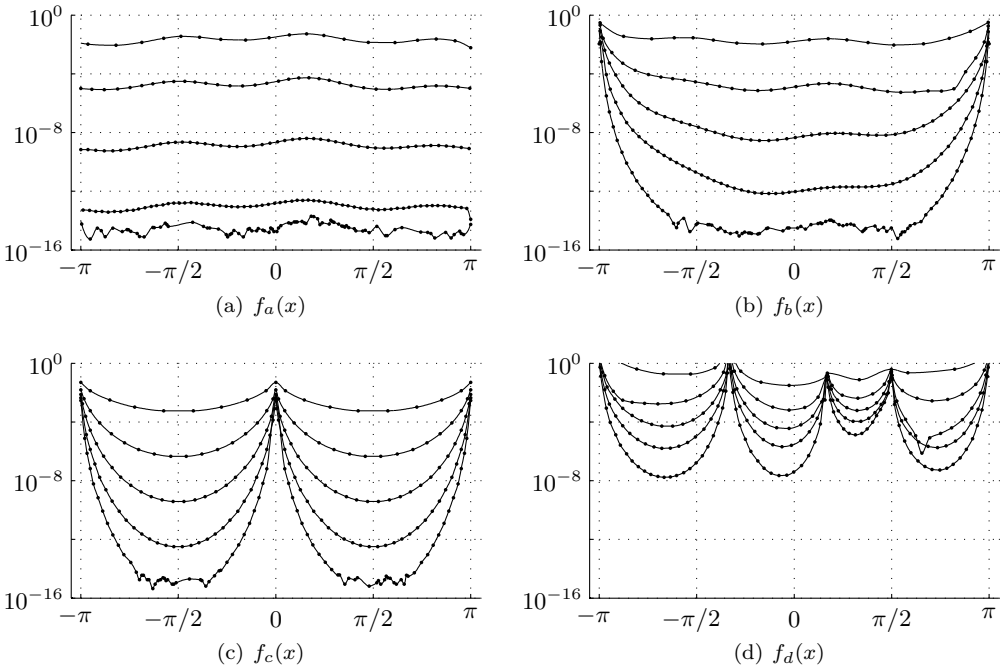

FIG. 3.1. *Error envelopes (see Figure 1.2 for explanation) of Fourier–Padé approximants for* $N = 8, 16, \ldots, 40$. *Away from jump points, spectral convergence is observed. Compare to Figure 1.2.*

by Brezinski [4] that FP-type approximants do converge faster at ordinary points than the partial sums.)

The relationship between Fourier partial sums and trigonometric interpolants is analogous to the relationship between Padé approximants and rational interpolants (also called multipoint Padé approximants). Thus the interpolation form of the Fourier–Padé technique, which we call *Fourier-rational interpolation* (FRI), is the approximation $p(z)/q(z)$, where polynomials p and q have degrees $N-1$ and N and satisfy

$$p(z_n) - y_n q(z_n) = 0, \qquad n = 0, \ldots, 2N-1, \tag{3.3}$$

where $z_n = e^{ix_n}$.

Figure 3.2 shows the results of Fourier rational interpolation for our four test functions. The results are qualitatively very similar to those in Figure 3.1 for the Fourier–Padé method.

4. Singularities and Fourier–Padé. Padé approximants are known to converge in the presence of discontinuities. This was shown for algebraic, bounded branch cuts in [13] and is also known for the unbounded cut along the negative real axis in the example of Figure 2.1(b). However, in that example it was observed that the jump in the function along the cut nevertheless makes approximation inaccurate in practice. It is not surprising that the Fourier–Padé method is shown in Figure 3.1 to have the same problem at jump locations; poles do not intrinsically reproduce jump behaviors.

Consider the classical example of $f(x) = x$, extended periodically from $[-\pi, \pi)$.

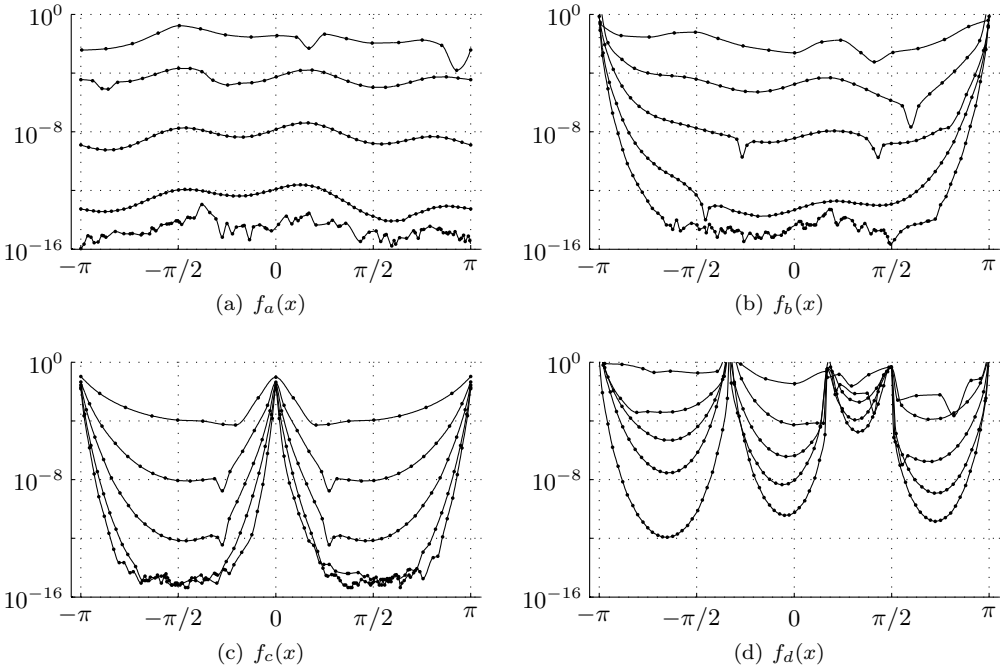

(a) $f_a(x)$ (b) $f_b(x)$

(c) $f_c(x)$ (d) $f_d(x)$

FIG. 3.2. *Error envelopes of Fourier–rational interpolants for* $16, 32, \ldots, 80$ *equispaced points. Away from jump points, spectral convergence is observed.*

For the functions f^+ and f^- defined in (1.2), we have

$$\begin{aligned} f^+(z) &= -i\left(z - \frac{z^2}{2} + \frac{z^3}{3} - \cdots\right) = -i\log(z+1). \\ f^-(z) &= i\left(z - \frac{z^2}{2} + \frac{z^3}{3} - \cdots\right) = i\log(z+1). \end{aligned} \tag{4.1}$$

Note that, in light of (1.3), on $|z| = 1$ we have

$$f^+(z) + f^-\big(z^{-1}\big) = f^+(z) + \overline{f^+(z)} = i\log\left(\frac{1+e^{-ix}}{1+e^{ix}}\right) = i\log e^{-ix} = x, \tag{4.2}$$

as required. By the linearity and shift properties of the Fourier transform, every zeroth-order (i.e., value) jump in a generic real f at the point $x = \xi$ can be attributed to a logarithm in f^+ of the form

$$\log\left(1 - \frac{z}{e^{i\xi}}\right), \tag{4.3}$$

with branch point at the corresponding location on the unit circle.

At this point it might seem promising to try to differentiate f^+ in order to convert logarithmic singularities into poles. These poles would then be well approximated by standard Padé methods. (See also [12] on series differentiation, and the "D-log approximant" of [1, p. 51]. We revisit the idea in section 6.) However, if f' is also discontinuous, it too can be expected to have logarithmic singularities in the z-plane. Instead, we shall look to incorporate logarithmic singularities into the approximation directly.

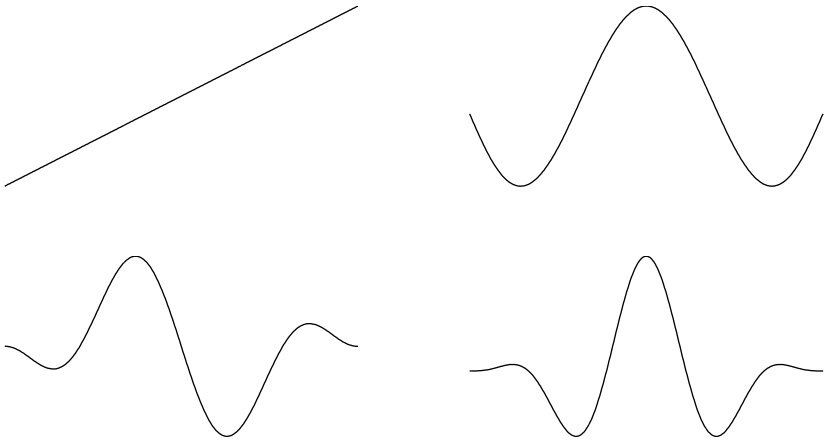

FIG. 4.1. *Real parts of the functions* $(-i)^{m+1}(1+z)^m \log(1+z)$ *for* $m = 0, 1, 2, 3$ *for* $z = e^{ix}$. *Each leads to a jump in the* m*th derivative at* $x = \pm\pi$.

We first consider a function which is C^0 but not differentiable; i.e., having a first-order jump. We could continue with $f(x) = x^2/2$ as a prototype:

$$f^+(z) = -z + \frac{1}{4}z^2 - \frac{1}{9}z^3 + \cdots = \mathrm{Li}_2(-z),$$

where Li_2 is the dilogarithm. It is far more convenient computationally, however, to observe that

$$f^+(z) = (1+z)\log(1+z) = z + \frac{1}{2}z^2 - \frac{1}{6}z^3 + \frac{1}{12}z^4 - \dots$$

also has a real part which is continuous on $|z| = 1$ and which satisfies

$$\frac{d}{dx}f^+(z) = iz\frac{d}{dz}f^+(z) = iz\left[1 + \log(1+z)\right].$$

After combination with its conjugate, this expression has a jump at $z = -1$ as required for a first-order singularity. In general, the real part of $f^+(z) = (-i)^{m+1}(1+z)^m \log(1+z)$ has an mth-order singularity, as illustrated in Figure 4.1. For other jump locations, this is easily shifted around the unit circle as in (4.3).

This observation suggests that to represent a function with jumps at all orders at $x = \xi$, we let

$$f^\pm(z) = g_0^\pm(z) + \sum_{m=0}^{\infty} R_m^\pm (z-\zeta)^m \log\Big(1 - \frac{z}{\zeta^{\pm 1}}\Big) = g_0^\pm(z) + g_1^\pm(z)\log\Big(1 - \frac{z}{\zeta^{\pm 1}}\Big), \quad (4.4)$$

where $\zeta = e^{i\xi}$ and $g_{0,1}^\pm$ are analytic near $z = -1$. This in turn suggests the modification of the Fourier–Padé method to

$$p^\pm(z) + r_1^\pm(z)\log(1 - z/\zeta_1^{\pm 1}) + \cdots + r_s^\pm(z)\log(1 - z/\zeta_s^{\pm 1}) = q^\pm(z)f^\pm(z) + O(z^{N+1}) \quad (4.5)$$

for singularities $\zeta_1, \dots, \zeta_s$ on the unit circle. We call this the *singular Fourier–Padé* (SFP) approximation. If $s = 0$, it is the standard Fourier–Padé method. We remark

again that for real functions, only the + superscript case need be computed. Note that dividing (4.5) through by $q^{\pm}(z)$ implies that the equivalents of g_0 and g_1 in (4.4) have a shared rational denominator. This choice is crucial to developing a practical algorithm in the next section.

It is interesting to consider how SFP works when applied to two of the most elegant and classical cases of the Gibbs phenomenon. First, for $f(x) = x$, we note from (4.1) that exact reconstruction using (4.5) occurs when $p^+ \equiv 0$, $q^+ \equiv 1$, and $r_1 \equiv -i$. In the case $f(x) = \text{signum}(x)$, we observe that the transformation $(1+z)/(1-z)$ maps the unit circle to the imaginary axis, and hence

$$f^+(z) = \frac{-i}{\pi} \log\left(\frac{1+z}{1-z}\right) \tag{4.6}$$

has real part equal to half of the signum function. With $\zeta_1 = -1$, $\zeta_2 = 1$ in (4.5), we again get exact reconstruction when p^+, q^+, and $r^+_{1,2}$ are constants.

In the case of rational interpolation as in (3.3), there is no longer a splitting of $f(z)$ into analytic and co-analytic parts. Hence we combine the terms $\log(1 - z/\zeta)$ and $\log(1 - \zeta/z)$ to get $-i\log(z/\zeta)$. The natural adaptation of (4.5), then, is

$$p(z_n) + r_1(z_n)\log(\zeta_1^{-1} z_n) + \cdots + r_s(z_n)\log(\zeta_s^{-1} z_n) - f_n q(z_n) = 0, \tag{4.7}$$

$$n = 0, \ldots, 2N-1. \tag{4.8}$$

The resulting approximation

$$f(x) \approx \frac{p(z) + r_1(z)\log(\zeta_1^{-1} z) + \cdots + r_s(z)\log(\zeta_s^{-1} z)}{q(z)}, \qquad z = e^{ix}. \tag{4.9}$$

is called the *singular Fourier–rational interpolant* (SFRI) for f

5. Singular Fourier–Padé algorithm. We take a straightforward approach to computing the polynomial coefficients needed in the SFP method. For clarity, we write out formulas in the case of $s = 1$ jump location at $x = \pm\pi$. Rewriting (4.5) (with some superscripts dropped for clarity), we have

$$p(z) + r(z)\log(1+z) = q(z) f^{\pm}(z) + O(z^{N+1}). \tag{5.1}$$

Both $\log(1+z)$ and $f^{\pm}(z)$ have Taylor expansions known to order N. Our goal is to derive a linear system for the unknown polynomial coefficients.

Note that $q(z)$ and $r(z)$ are determined by the terms of order greater than n_p alone. Thus we seek a solution to

$$\begin{bmatrix} C & -L \end{bmatrix} \begin{bmatrix} \mathbf{q} \\ \mathbf{r} \end{bmatrix} = \mathbf{0}. \tag{5.2}$$

Here C is the $(n_q + n_r + 1) \times (n_q + 1)$ Toeplitz matrix

$$\begin{bmatrix} c_{N/2+1} & c_{N/2} & \cdots & c_1 \\ c_{N/2+2} & c_{N/2+1} & \cdots & c_2 \\ \vdots & \vdots & & \vdots \\ c_N & c_{N-1} & \cdots & c_{N/2} \end{bmatrix}, \tag{5.3}$$

and L has size $(n_q + n_r + 1) \times (n_r + 1)$ and is defined similarly using the Taylor coefficients of $\log(1+z)$. The vectors $\mathbf{q}$ and $\mathbf{r}$ hold the unknown polynomial coefficients

in order of increasing degree. Because the matrix in (5.2) has column dimension one greater than its row dimension, at least one nonzero solution exists. Usually this can be made into a square system by choosing, say, $q(0) = 1$, but if one does not want to assume that any particular coefficient is nonzero, one can solve (5.2) by a singular value decomposition. Finally, the coefficients of $p(z)$ are found by multiplication, via

$$\mathbf{p} = \begin{bmatrix} \frac{1}{2}c_0 & 0 & \cdots & 0 \\ c_1 & \frac{1}{2}c_0 & \cdots & 0 \\ \vdots & \vdots & & \vdots \\ c_{N/2} & c_{N/2-1} & \cdots & \frac{1}{2}c_0 \end{bmatrix} \mathbf{q} - \begin{bmatrix} \ell_0 & 0 & \cdots & 0 \\ \ell_1 & \ell_0 & \cdots & 0 \\ \vdots & \vdots & & \vdots \\ \ell_{N/2} & \ell_{N/2-1} & \cdots & \ell_0 \end{bmatrix} \mathbf{r}. \tag{5.4}$$

If the original function f is real, only f^+ needs to be considered in (5.1). If there is more than one jump location in the interval and (4.5) is to be used, the equation (5.2) is modified to have an L matrix and a vector of coefficients for each location, and (5.4) changes similarly.

We have no rigorously optimal formula for choosing the degrees n_p, n_q, and $n_r^{(1)}, \ldots, n_r^{(s)}$. Because the denominator polynomial $q(z)$ is shared, we allow n_q to be the largest, with the others equal so far as possible. For the case of just one jump location, taking n_q at roughly 40% of the total available degrees of freedom seems to work well. Experiments suggest that these choices can affect the observed accuracy, occasionally by as much as an order of magnitude, but on average there is little variation within a broad range of choices.

The heart of the algorithm is implemented in MATLAB code as shown in Figure 5.1. The `padelog` function shown in the figure would be called twice, for f^+ and f^- (unless f is real, in which case once call suffices). Figure 5.2 shows how `padelog` could be used on our example $f_c(x) = |x|$. The resulting graph (not shown) demonstrates almost no visible difference between f_c and its singular Fourier–Padé approxmation using the first seven nonzero Fourier coefficients.

In Figure 5.3 we show the errors resulting when SFP is applied to our four test functions. The convergence of the SFP approximations appears to be globally spectral, albeit not at a spatially uniform rate. (Convergence at a zeroth-order jump is to the average of the one-sided limit values.) The convergence at a jump is limited somewhat by the well-known numerical ill-conditioning of the straightforward Padé problem. Figure 5.4 shows that in arbitrary-precision arithmetic, convergence at $\pm\pi$ for the nonperiodic function f_b is spectral down to at least 10^{-16}.

The interpolation case similarly reduces to a linear problem. Let V_M be a Vandermonde matrix of degree M; that is,

$$V_{nm} = (z_n)^m, \qquad n = 0, \ldots, 2N-1, \quad m = 0, \ldots, M.$$

The coefficients of the polynomials in (4.7) satisfy an equation of the form

$$\begin{bmatrix} V_{n_p} & -\operatorname{diag}(f_0, \ldots, f_{2N-1}) V_{n_q} & L_1 V_{n_1} & \cdots & L_s V_{n_s} \end{bmatrix} \begin{bmatrix} \mathbf{p} \\ \mathbf{q} \\ \mathbf{r}_1 \\ \vdots \\ \mathbf{r}_s \end{bmatrix} = \mathbf{0}.$$

The matrix has column dimension one larger than row dimension, so a nonzero solution exists. Results on our four test examples are shown in Figure 5.5. The improvement close to the jump locations is especially significant.

```
function [p,q,r] = padelog(c,z0)
%   PADELOG(c,z0) finds an expansion of the form
%
%      p(z) +  r{1}(z) log(1-z/z0(1)) + ... + r{m}(z) log(1-z/z0(m))
%     ------------------------------------------------------------
%                              q(z)
%
%                        N+1
%          =  f(z) + O(z   ),  z->0
%
%   for polynomials p, q, r{1},..., r{m}. Here f(z) is a  polynomial
%   of degree N, whose coefficients are given in ascending degree in
%   c. The points in vector z0 represent the locations of jumps in f.

N = length(c)-1;
m = length(z0);

% Figure out the degrees of the polynomials.
nq = ceil((N-m)/(m+1.5));
s = floor((N-m-nq)/(m+1));
nr = s*ones(1,m);
np = N-m-nq-sum(nr);

% Taylor coeffs of log terms
k = (1:N)';
for s = 1:m
  l{s} = [0;-1./(k.*z0(s).^k)];
end

% The polynomials q and r{:} are found from the highest-order coeffs
row = [c(np+2:-1:max(1,np-nq+2)); zeros(nq-np-1,1)];
C = toeplitz(c(np+2:N+1),row);
L = cell(1,m);
for s = 1:m
  row = [l{s}(np+2:-1:max(1,np-nr(s)+2));zeros(nr(s)-np-1,1)];
  L{s} = toeplitz(l{s}(np+2:N+1),row);
end

% Find a vector v satisfying [C -L{1} ... -L{m}]*v = 0
Z = null(cat(2,-C,L{:}));   % vector(s) in nullspace
qr = Z(:,end);
qr = qr/qr(min(find(qr)));  % normalization

% Pull out polynomials
q = qr(1:nq+1);
idx = nq+1;
r = cell(1,m);
for s = 1:m
  r{s} = qr(idx+(1:nr(s)+1));
  idx = idx + nr(s)+1;
end

% Remaining polynomial is found using low-order terms
C = toeplitz(c(1:np+1),[c(1) zeros(1,nq)]);
p = C*q;
for s = 1:m
  L = toeplitz(l{s}(1:np+1),[l{s}(1) zeros(1,nr(s))]);
  p = p - L*r{s};
end
```

FIG. 5.1. *Code for finding the polynomials in* (4.5) *for the singular Fourier–Padé method.*

```
c = [pi/4 zeros(1,11)];
c(2:2:12) = -(2/pi)*(1:2:11).^(-2);
z0 = exp(1i*[-pi 0]);
[p,q,r] = padelog(c,z0);

x = linspace(-pi+10*eps,pi-10*eps,200);  z = exp(1i*x);
pz = polyval(p(end:-1:1),z);
qz = polyval(q(end:-1:1),z);
rz{1} = polyval(r{1}(end:-1:1),z);
rz{2} = polyval(r{2}(end:-1:1),z);
fplus = ( pz + rz{1}.*log(1-z/z0(1)) + rz{2}.*log(1-z/z0(2)) ) ./ qz;
plot(x,abs(x),x,2*real(fplus),'k.')
```

FIG. 5.2. *Demonstration of using the code of Figure 5.1 on the function* $f_c(x) = |x|$.

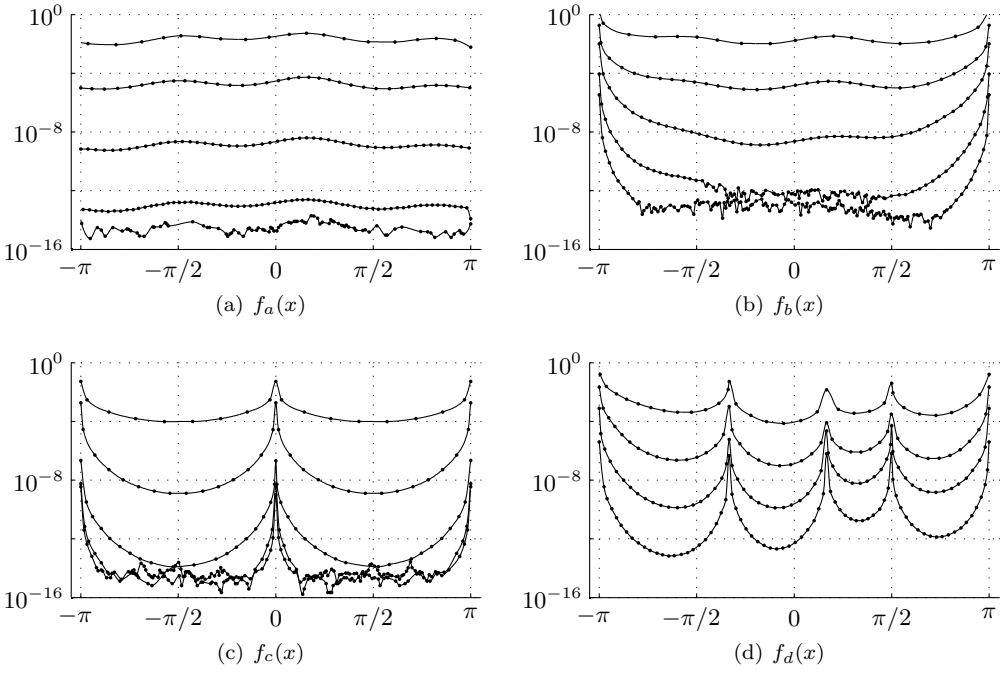

(a) $f_a(x)$ (b) $f_b(x)$

(c) $f_c(x)$ (d) $f_d(x)$

FIG. 5.3. *Error envelopes of singular Fourier–Padé approximants for* $N = 8, 16, \ldots, 40$ *(except in the last example, when the* $N = 8$ *case is not defined). Compare to Figure 3.1.*

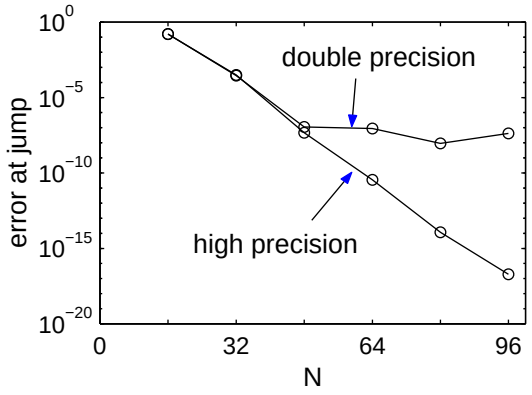

FIG. 5.4. *Error at the jump singularity using SFP for the function f_b. Using arbitrarily high precision (as performed by Mathematica), the convergence is spectral. For a double-precision implementation, the effects of Padé ill-conditioning ultimately limit the accuracy obtained.*

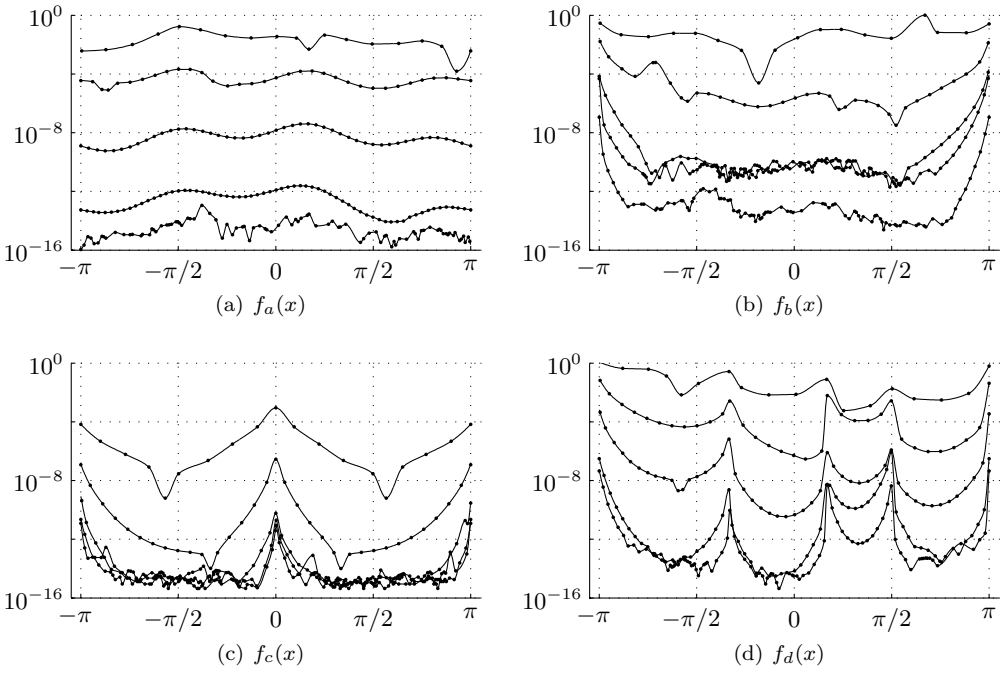

FIG. 5.5. *Error envelopes of singular Fourier–rational interpolants for* $16, 32, \ldots, 80$ *equispaced points. Compare to Figure 3.2.*

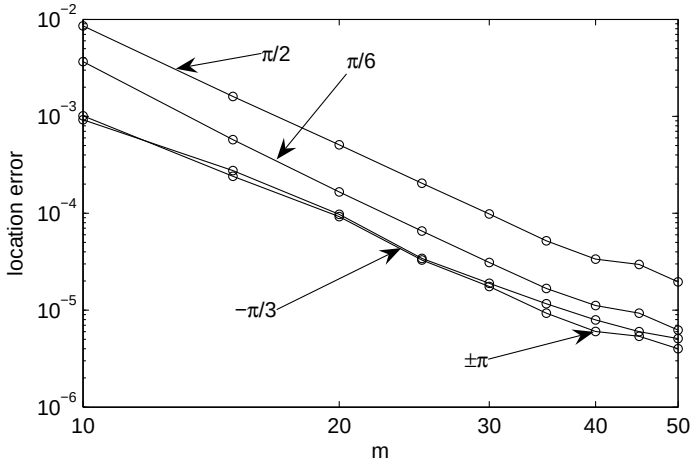

FIG. 6.1. *Errors in the four jump locations of the function f_d, as found by Fourier–Padé approximations of type $[m, m]$ to the derivative. The convergence is roughly $O(m^{-4})$.*

6. Locating singularities. The methods described above all assume that the locations of all irregular points are known. But we can also use Padé ideas to estimate the locations of jumps well enough to allow good reconstruction nearly everywhere in the interval.

As observed in section 4 after formula (4.1), differentiation of a function with a jump in value leads to an ordinary pole at the jump location. Referring to (1.2) and recalling that $\frac{d}{dx} = iz\frac{d}{dz}$, this suggests that we find Padé approximations of

$$g_N^+(z) = \sum_{n=0}^{N} inc_n z^n, \quad g_N^-(z) = \sum_{n=0}^{N} -inc_{-n} z^n. \tag{6.1}$$

While higher-order jumps mean that $g^\pm$ still have logarithmic singularities that make the Padé approximations imperfect near the jumps, we can hope that the poles of the resulting approximations nevertheless are good indicators of the jump locations, which can then be incorporated into a singular Fourier–Padé approximation.

Figure 6.1 indicates how well this works on the function f_d having jumps at $\pm\pi$, $-\pi/3$, $\pi/6$, and $\pi/2$. We form diagonal Padé approximations of type $[m, m]$ to the differentiated function (6.1), and a pole whose magnitude is within 0.01 of the unit circle is assumed to be a jump location (after projection onto the circle). For $m = 5$ only the jump at $-\pi/3$ is noticed by this method, but for $m = 10, 15, \ldots, 50$, the method suggests exactly four jump locations whose errors are shown in the figure. The two larger jumps are located a bit more accurately than the weaker ones. The error seems to vary roughly as $O(m^{-4}) = O(N^{-4})$. This compares very favorably to the $O(\log N/N)$ error expected by filtering methods described in [9] and is only slightly less accurate than the best cases reported using the more complicated method in [7]. Figure 6.2 shows the result of SFP approximation with the jump locations found using $m = 20$. The results are noticeably better than for Fourier–Padé (Figure 3.1) but not as good as SFP with the exact jump locations (Figure 5.3). Of course, values at the jumps themselves cannot be reconstructed accurately using erroneous locations. Figure 6.3 shows the error in the vicinity of the jump at $x = \pi/6$.

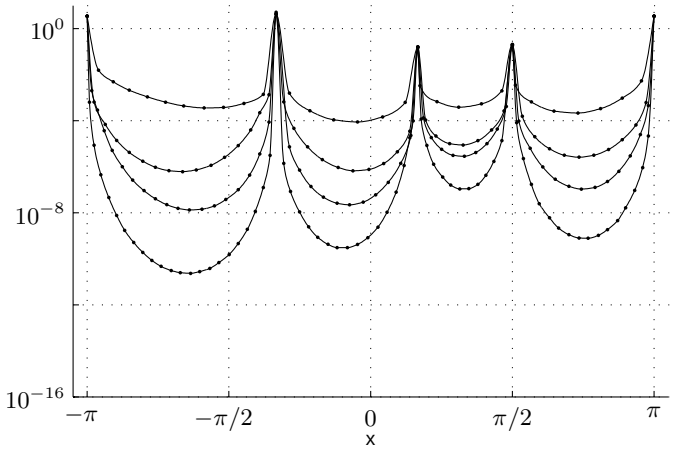

FIG. 6.2. *Error envelopes for singular Fourier–Padé approximations of f_d with $N = 16, 24, \ldots, 40$, using differentiated Fourier–Padé approximations to estimate the jump locations. Compare to Figures 3.1 and 5.3.*

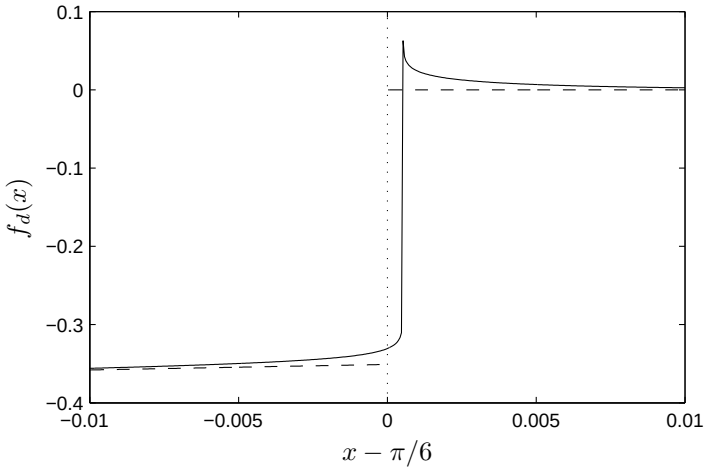

FIG. 6.3. *Approximation of f_d (shown with dashed curves) near $x = \pi/6$ using $N = 40$ and an estimated jump location.*

For the interpolation problem, we can use the aliased coefficients (1.5) computed by the FFT to construct a differentiated Fourier–Padé approximation. This in turn suggests singularity locations to be used in (4.9). For our test function f_d, however, we found that aliasing decreases the accuracy of the estimated jump locations. For values of N from 40 to 100 (using diagonal Fourier–Padé approximants of maximum degree $[N/2, N/2]$), we find that the location error stays fairly constant between 10^{-2} and 10^{-3}. Algorithmically, all that would seem to matter is that the jump be located between the correct pair of nodes, but this failed for the jumps at $\pm\pi$ and $\pi/2$. In Figure 6.4 we find that the SFRI approximations do not improve on ordinary rational interpolation.

7. Conclusions. Fourier–Padé approximation makes a dramatic improvement over the direct partial summation of Fourier series. Convergence is accelerated even

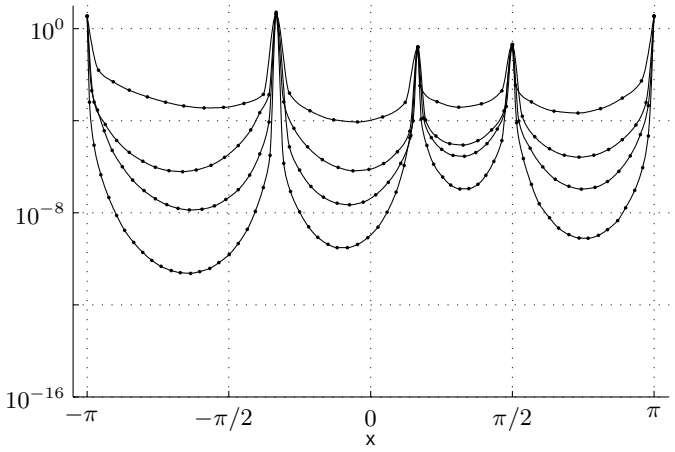

FIG. 6.4. *Error envelopes for singular Fourier–rational interpolation approximations of f_d with $N = 32, 48, \ldots, 80$ nodes. The jump locations were estimated using differentiated aliased Fourier–Padé approximations based on $N = 60$. Compare to Figures 3.2 and 5.5.*

for analytic, periodic functions, and the global effects of the Gibbs phenomenon due to a jump are largely eliminated. Moreover, this improvement is available via standard Padé approximation, so that better numerical methods than the direct linear algebra described above are available [1, Chapter 3]. Equally impressive results are observed when rational interpolation is used in place of trigonometric polynomials.

In order to reconstruct functions at and near jumps, however, a more careful treatment is beneficial. The Gibbs phenomenon is manifested in the complex plane by logarithmic branches that can, when their locations are known, be incorporated directly into Padé-type approximations. These appear to converge globally and exponentially, offering 4–6 digits of accuracy at the jumps with just 40 terms of the series of difficult functions. Similar results obtain in the interpolation problem.

When jump locations are not known in advance, they too can be found through Padé approximation, after differentiation of the series. In the truncated series case, the results are observed to be about fourth-order accurate, which compares favorably with existing methods. The interpolation case is less successful, and one might be better served by less accurate but more robust local detection techniques.

We view the main opportunity offered by our approach to be in situations when Fourier reconstruction is desired for intrinsically nonperiodic data. Traditional spectrally accurate representations would in such cases typically be based on Chebyshev or similar orthogonal polynomials. However, these are associated with highly nonuniform data point locations, which may be suboptimal for some functions and which are seldom natural or practical in connection with experimental data. The singular Padé approach allows many such difficulties to be bypassed, as it creates an easily calculated, global, and spectrally accurate approximation to periodic and nonperiodic functions to be constructed from a relatively small number of their leading Fourier coefficients.

REFERENCES

[1] G. A. Baker and P. Graves-Morris, *Padé Approximants*, vol. 59, Cambridge University Press, 2nd ed., 1996.
[2] C. M. Bender and S. A. Orszag, *Advanced Mathematical Methods for Scientists and Engineers*, Springer, 1997.
[3] J. P. Boyd, *Trouble with Gegenbauer reconstruction for defeating Gibbs' phenomenon: Runge phenomenon in the diagonal limit of Gegenbauer polynomial approximations*, J. Comput. Phys., 204 (2005), pp. 253–264.
[4] C. Brezinski, *The asymptotic behavior of sequences and new series transformations based on the Cauchy product*, Rocky Mountain J. Math., 21 (1991), pp. 71–84.
[5] J. S. R. Chisholm and A. K. Common, *Generalisations of Padé approximation for Chebyshev and Fourier series*, in E. B. Christoffel: The Influence of His Work on Mathematics and the Physical Sciences, P. L. Butzer and F. Fehér, eds., Birkhäuser, 1981, pp. 212–231.
[6] T. A. Driscoll and B. Fornberg, *A Padé-based algorithm for overcoming the Gibbs phenomenon*, Numer. Alg., 26 (2001), pp. 77–92.
[7] K. S. Eckhoff, *On a high order numerical method for functions with singularities*, Math. Comp., 67 (1998), pp. 1063–1087.
[8] J. F. Geer, *Rational trigonometric approximations using Fourier series partial sums*, J. Sci. Computing, 10 (1995), pp. 325–356.
[9] A. Gelb and E. Tadmor, *Detection of edges in spectral data II. Nonlinear enhancement*, SIAM J. Numer. Anal., 38 (2000), pp. 1389–1408.
[10] D. Gottlieb and C.-W. Shu, *On the Gibbs phenomenon and its resolution*, SIAM Review, 39 (1997), pp. 644–668.
[11] W. B. Gragg, *Laurent, Fourier, and Chebyshev–Padé tables*, in Padé and Rational Approximation, Theory and Applications, E. B. Saff and R. S. Varga, eds., Academic Press, 1977.
[12] G. Kvernadze, T. Hagstrom, and H. Shapiro, *Locating discontinuities of a bounded function by the partial sums of its Fourier series*, J. Sci. Comput., 14 (1999), pp. 301–327.
[13] J. Nuttall and S. R. Singh, *Orthogonal polynomials and Padé approximants associated with a system of arcs*, J. Approximation Theory, 21 (1977), pp. 1–42.
[14] B. D. Shizgal and J.-H. Jung, *Towards the resolution of the Gibbs phenomena*, J. Comput. Appl. Math., 161 (2003), pp. 41–65.
[15] A. Sidi, *Practical Extrapolation Methods*, Cambridge University Press, 2003.
[16] R. D. Small and R. J. Charron, *Continuous and discrete nonlinear approximation based on Fourier series*, IMA J. Num. Analy., 8 (1988), pp. 281–293.
[17] J. Tanner, *Optimal filter and mollifier for piecewise smooth spectral data*. Electronically published on January 23, 2006, 2006. S 0025-5718(06)01822-9.
[18] L. N. Trefethen, *Spectral Methods in MATLAB*, Society for Industrial and Applied Mathematics, 2000.